Research Article | Vol. 27, No. 4 | 18 Feb 2019 | OPTICS EXPRESS 3963
Optics EXPRESS

Pseudo-Schell model sources

J. C. G. DE SANDE,[1,*] ROSARIO MARTÍNEZ-HERRERO,[2] GEMMA PIQUERO,[2] MASSIMO SANTARSIERO,[3] AND FRANCO GORI[3]

[1] *ETSIS de Telecomunicación, Universidad Politécnica de Madrid, Campus Sur, 28031 Madrid, Spain*
[2] *Departamento de Óptica, Universidad Complutense de Madrid, Ciudad Universitaria, 28040 Madrid, Spain*
[3] *Dipartimento di Ingegneria, Università Roma Tre, Via V. Volterra 62, 00146 Rome, Italy*
[*] *jcgsande@ics.upm.es*

Abstract: Partially coherent pseudo-Schell model sources are introduced and analyzed. They present radial symmetry and coherence characteristics depending on the difference between the radial distances of two points from the source center. As a consequence, all points belonging to circles centered on the symmetry center of the source are perfectly correlated. We show that such sources radiate fields with peculiar behaviors in paraxial propagation. In particular, when compared to beams produced by Gaussian Schell-model sources with comparable coherence parameters, the irradiance can present sharper profiles and higher peak values and a better beam quality parameter. Furthermore, when a pseudo-Schell model source presents a vortex, the propagated beam preserves a null of the intensity along its axis.

1. Introduction

The coherence characteristics of a light source affect the properties of the propagated field and, in particular, its irradiance profile, so that it is also possible to tune the beam shape by controlling the coherence of the source [1–9]. Such a feature is of a great interest in those applications, such as in remote sensing [10], free space optical communications [11–13], or optical trapping [14, 15], just to mention some examples where the use of partially coherent sources have been proposed, due to the advantages they present if compared to their coherent counterparts.

The coherence properties of scalar sources are appropriately described by the cross-spectral density (CSD) function [1], which gives account of the correlations, in the space-frequency domain, between the field at two different points at the source plane. When a source presents shift-invariant coherence properties, it is adequately described by the so called Schell model. Schell-model sources often represent a useful model to treat natural sources but have also the advantage that they can always be synthesized starting from planar spatially incoherent sources with suitable irradiance profile [1, 16–23]. Among them, Gaussian Schell-model (GSM) sources, where both the spectral degree of coherence and the irradiance profile are Gaussianly shaped [1, 24], have been extensively studied and characterized [25–32]. Since the publication of the superposition rule [33, 34], that have eased the design of physically realizable CSD's, different kind of sources, of the Schell-model type [20, 21, 35, 36] or not [6, 37–45] have been proposed.

In this work, a class of partially coherent planar sources is proposed and characterized. In particular, we examine radially symmetric planar sources, whose coherence characteristics between two points depend on the difference between the radial distances of these two points from the symmetry center. Therefore, it turns out that all points belonging to circles centered on the symmetry center are perfectly correlated. Because of the dependence on the difference of radial coordinates of the two considered points, such sources will be called pseudo-Schell model sources [46]. Different classes of pseudo-Schell model sources can be obtained by changing the functional dependence on the above difference. Characteristics of this type of sources are studied for some particular cases, and coherence and irradiance features of the propagated field

#352855 https://doi.org/10.1364/OE.27.003963
Journal © 2019 Received 27 Nov 2018; revised 11 Jan 2019; accepted 12 Jan 2019; published 4 Feb 2019

Optics EXPRESS

are presented, together with some global parameters, such as the beam quality and the beam size evolution.

2. Pseudo Schell-model sources

The CSD function $W(\boldsymbol{\rho}_1, \boldsymbol{\rho}_2, 0)$ is an appropriate tool for describing in the space-frequency domain stochastic, statistically stationary up to second order, light sources [1], and expresses the correlation of the field at two arbitrary positions across the source plane. Here, we denote by $\boldsymbol{\rho}_j$ (with $j = 1, 2$) the transverse position vectors of the two points and suppose that the source lies on the plane $z = 0$. The dependence on the temporal frequency is omitted for brevity. In the following, both rectangular (ξ, η) and polar (ρ, φ) coordinates will be used for the vector $\boldsymbol{\rho}$.

The CSD of a physically realizable source must satisfy the non-negativeness condition [1]. While directly checking such condition for a given cross-spectral density is often not an easy task, a necessary and sufficient condition to devise genuine CSDs was established some years ago [33, 34]. In the following, use will be made of such a rule.

Let us consider a light source described by a CSD function of the following form:

$$W(\boldsymbol{\rho}_1, \boldsymbol{\rho}_2, 0) = \tau^*(\boldsymbol{\rho}_1)\,\tau(\boldsymbol{\rho}_2) \int A^*(\boldsymbol{\rho}_1, \boldsymbol{\upsilon})\,A(\boldsymbol{\rho}_2, \boldsymbol{\upsilon})\,\mathrm{d}\boldsymbol{\upsilon} \tag{1}$$

where $*$ denotes complex conjugation, $\tau(\boldsymbol{\rho})$ is a general complex function, and

$$A(\boldsymbol{\rho}, \boldsymbol{\upsilon}) = H(\upsilon)\exp(\mathrm{i}k\rho\upsilon\cos\psi)\,, \tag{2}$$

with k being the wavenumber, $\boldsymbol{\upsilon}$ a vector with polar coordinates (υ, ψ), and H an arbitrary function of υ. In physical terms, the CSD in Eq. (1) is obtained as the incoherent superposition of a continuous set of perfectly coherent beams (parametrized by the vector $\boldsymbol{\upsilon}$), whose amplitudes are multiplied by the transmission function of a conical lens [47, 48]. Due to the way in which $W(\boldsymbol{\rho}_1, \boldsymbol{\rho}_2, 0)$ has been constructed, it represents a genuine CSD matrix [34, 49, 50].

Substitution of Eq. (2) into Eq. (1) gives

$$W(\boldsymbol{\rho}_1, \boldsymbol{\rho}_2, 0) = \tau^*(\boldsymbol{\rho}_1)\,\tau(\boldsymbol{\rho}_2)\,g(\rho_2 - \rho_1)\,, \tag{3}$$

where

$$g(\rho) = 2\pi \int_0^\infty |H(\upsilon)|^2\,J_0(k\rho\upsilon)\,\upsilon\,d\upsilon\,, \tag{4}$$

and $J_\nu(\cdot)$ is the Bessel function of first kind and order ν [51]. It can be observed that the irradiance of the source, $I(\boldsymbol{\rho}, 0) = W(\boldsymbol{\rho}, \boldsymbol{\rho}, 0)$, depends on $\tau(\boldsymbol{\rho})$, while its coherence properties are determined by the function g, since [1]

$$\mu(\boldsymbol{\rho}_1, \boldsymbol{\rho}_2, 0) = \frac{W(\boldsymbol{\rho}_1, \boldsymbol{\rho}_2, 0)}{\sqrt{W(\boldsymbol{\rho}_1, \boldsymbol{\rho}_1, 0)\,W(\boldsymbol{\rho}_2, \boldsymbol{\rho}_2, 0)\}}} = \frac{\tau^*(\boldsymbol{\rho}_1)\,\tau(\boldsymbol{\rho}_2)}{|\tau(\boldsymbol{\rho}_1)\,\tau(\boldsymbol{\rho}_2)|}\,g(\rho_2 - \rho_1)\,, \tag{5}$$

whose absolute value only depends on the difference between the radial distances of the considered points from the source center. Without loss of generality, in deriving Eq. (5) we assumed $g(0) = 1$, obtained by suitably normalizing $H(\upsilon)$. Sources of this kind will be called pseudo Schell-model sources.

Note that Eqs. (3) and (4) define a whole class of sources whose coherence properties depend only on the radial distance difference of the two considered points (except for a possible phase factor). A new family of sources of this class is generated just by changing $H(\upsilon)$. Once a function $H(\upsilon)$ is chosen, different behaviors can be found depending on the shape of $\tau(\boldsymbol{\rho})$.

Optics EXPRESS

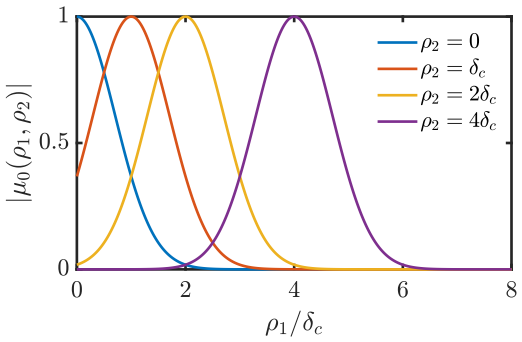

Fig. 1. Absolute value of the spectral degree of coherence along a radius and relative to a point at different distances ρ_2 from the source center.

3. Pseudo Schell-model sources with Gaussian degree of coherence

To illustrate some properties of pseudo Schell-model sources, let us consider a particular choice of $H(\upsilon)$, i.e.,

$$H(\upsilon) = \frac{k\delta_c}{2\sqrt{\pi}} \exp\left(-\frac{1}{8}k^2\delta_c^2\upsilon^2\right), \tag{6}$$

where the factor $k\delta_c/2\sqrt{\pi}$ has been introduced in order to get $g(0) = 1$, and δ_c is a real positive parameter. The latter defines the coherence properties of the source and, as it will be shortly seen, represents a measure of the width of a ring concentric to the source center where the degree of coherence is significant. We will refer to δ_c as the coherence parameter of the source.

Substituting from Eq. (6) into Eqs. (4) and (5) yields [51]

$$|\mu(\boldsymbol{\rho}_1, \boldsymbol{\rho}_2, 0)| = |g(\rho_2 - \rho_1)| = \exp\left[-\frac{(\rho_2 - \rho_1)^2}{\delta_c^2}\right]. \tag{7}$$

The absolute value of the degree of coherence reaches its maximum value of 1 for $\rho_1 = \rho_2$, that is, along rings concentric to the source center, and monotonically decreases on increasing $|\rho_2 - \rho_1|$. Figure 1 shows the shape of the absolute value of the degree of coherence as a function of ρ_1 for different values of ρ_2. A two-dimensional plot of $|\mu|$ is shown in Fig. 2 as a function of $\boldsymbol{\rho}_1$ for different values of $\boldsymbol{\rho}_2$. It presents circular symmetry and reduces to a twodimensional Gaussian function when $\boldsymbol{\rho}_2 = 0$. In such a case δ_c coincides with the standard deviation of the Gaussian, so that its squared modulus can be taken as a measure of the coherence area of the source around that point. On moving $\boldsymbol{\rho}_2$ away from the center, $|\mu|$ takes a donut-like shape with radius ρ_2 and width of the order of δ_c. When ρ_2 is significantly greater than δ_c the coherence area of the source can be taken of the order of $2\pi\rho_2\delta_c$.

Once the analytical expression of $H(\upsilon)$ is chosen, different sources are obtained on changing the modulating function $\tau(\boldsymbol{\rho})$. To get more information about properties that can be found for these families of sources, we choose τ as a Laguerre–Gaussian function [52] in which the Laguerre polynomial has order zero, that is,

$$\tau(\boldsymbol{\rho}) = A_0 \left(\frac{\sqrt{2}\,\rho}{w_0}\right)^m \exp\left(-\frac{\rho^2}{w_0^2}\right) \exp(\mathrm{i}m\varphi), \tag{8}$$

where A_0 is an amplitude factor, m an integer, and w_0 a positive quantity related to the source width. It reduces to a Gaussian function when $m = 0$ and, when $m \neq 0$, presents a donut-like

Optics EXPRESS

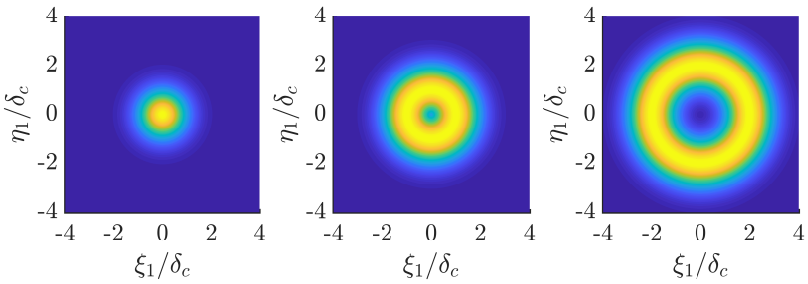

Fig. 2. Absolute value of the spectral degree of coherence relative to a point at distance $\rho_2 = 0$ (left), $\rho_2 = \delta_c$ (center) and $\rho_2 = 2\delta_c$ (right), from the source center.

shape and a phase vortex of charge m. We will denote by $W_m(\boldsymbol{\rho}_1, \boldsymbol{\rho}_2, 0)$ the resulting cross spectral densities, which take the form

$$W_m(\boldsymbol{\rho}_1, \boldsymbol{\rho}_2, 0) = I_0 \left(\frac{2\rho_1\rho_2}{w_0^2}\right)^m \exp\left(-\frac{\rho_1^2+\rho_2^2}{w_0^2}\right) \exp\left[-\frac{(\rho_2-\rho_1)^2}{\delta_c^2}\right] \exp\left[\mathrm{i}m(\varphi_2-\varphi_1)\right], \quad (9)$$

with $I_0 = |A_0|^2$. For brevity, we will call VGPSM (for Vortex Gaussian Pseudo-Schell-Model) sources, the sources described by the CSD in Eq. (9) or, for the specific case of $m = 0$, GPSM (for Gaussian Pseudo-Schell-Model) sources.

The results obtained for sources of this kind will be compared to the ones obtained from the corresponding (standard) Gaussian Schell-model sources with a vortex, i.e., [18, 53]

$$W_m^{(\mathrm{s})}(\boldsymbol{\rho}_1, \boldsymbol{\rho}_2, 0) = I_0 \left(\frac{2\rho_1\rho_2}{w_0^2}\right)^m \exp\left(-\frac{\rho_1^2+\rho_2^2}{w_0^2}\right) \exp\left[-\frac{(\boldsymbol{\rho}_2-\boldsymbol{\rho}_1)^2}{\delta_c^2}\right] \exp\left[\mathrm{i}m(\varphi_2-\varphi_1)\right], \quad (10)$$

where the degree of coherence depends on $|\boldsymbol{\rho}_2 - \boldsymbol{\rho}_1|$, instead of $\rho_2 - \rho_1$. Such sources will be denoted by GSM (when $m = 0$) or VGSM (for Vortex GSM, when $m \neq 0$) sources.

4. Propagation

To study the characteristics of the field upon free-space propagation we assume paraxial approximation and propagation direction along the z axis. Then, the Fresnel diffraction integral allows to obtain the CSD at any plane z = constant as [1]

$$W(\mathbf{r}_1, \mathbf{r}_2, z) = \frac{k^2}{4\pi^2 z^2} \iint W(\boldsymbol{\rho}_1, \boldsymbol{\rho}_2, 0) \exp\left[-\frac{\mathrm{i}k}{2z}\left(|\mathbf{r}_1-\boldsymbol{\rho}_1|^2 - |\mathbf{r}_2-\boldsymbol{\rho}_2|^2\right)\right] \mathrm{d}\boldsymbol{\rho}_1 \mathrm{d}\boldsymbol{\rho}_2, \quad (11)$$

where $\mathbf{r}_j = (x_j, y_j) = (r_j, \theta_j)$ (with $j = 1, 2$) are two typical position vectors across the transverse plane.

Optics EXPRESS

For the case of the CSD in Eq. (9), the integral in Eq. (11) gives

$$W(\mathbf{r}_1,\mathbf{r}_2,z) = \frac{2\pi I_0}{\lambda^2 z^2}\exp\left[\frac{\mathrm{i}k}{2z}\left({r_2}^2-{r_1}^2\right)\right]\exp\left[\mathrm{i}m\left(\theta_2-\theta_1\right)\right]$$

$$\times\int_0^\infty\int_0^\infty\left(\frac{2\,\rho_1\rho_2}{w_0^2}\right)^m\exp\left(-\frac{\rho_1^2+\rho_2^2}{w_0^2}\right)\exp\left[-\frac{(\rho_2-\rho_1)^2}{\delta_c^2}\right] \tag{12}$$

$$\times\exp\left[\frac{\mathrm{i}k}{2z}\left({\rho_2}^2-{\rho_1}^2\right)\right]J_m\left(\frac{k}{z}r_1\rho_1\right)J_m\left(\frac{k}{z}r_2\rho_2\right)\rho_1\rho_2\mathrm{d}\rho_1\mathrm{d}\rho_2\,,$$

which allows to evaluate the irradiance profile and the degree of coherence of the propagated field across any transverse plane. Eq. (12) will be numerically evaluated for the cases $m = 0$ and $m = 1$ and results will be shown in Section 5.

An alternative way to characterize the properties of the propagated field is convenient. One possibility is by means of some global parameters, such as the beam width and the beam divergence, that can be calculated from the expression of CSD of the source, i.e. at $z = 0$. These parameters can be expressed in terms of the second order moments of the beam, that in Cartesian coordinates read [54]

$$\begin{aligned}
\langle\xi^2\rangle &= \frac{1}{P}\iint\xi^2\,W(\xi,\eta;\xi,\eta;0)\,\mathrm{d}\xi\,\mathrm{d}\eta\,,\\
\langle\eta^2\rangle &= \frac{1}{P}\iint\eta^2\,W(\xi,\eta;\xi,\eta;0)\,\mathrm{d}\xi\,\mathrm{d}\eta\,,\\
\langle u^2\rangle &= \frac{1}{k^2P}\iint\left.\frac{\partial^2 W(\xi_1,\eta_1;\xi_2,\eta_2;0)}{\partial\xi_1\partial\xi_2}\right|_{\xi_1=\xi_2=\xi,\,\eta_1=\eta_2=\eta}\mathrm{d}\xi\,\mathrm{d}\eta\,,\\
\langle v^2\rangle &= \frac{1}{k^2P}\iint\left.\frac{\partial^2 W(\xi_1,\eta_1;\xi_2,\eta_2;0)}{\partial\eta_1\partial\eta_2}\right|_{\xi_1=\xi_2=\xi,\,\eta_1=\eta_2=\eta}\mathrm{d}\xi\,\mathrm{d}\eta\,,\\
\langle\xi u\rangle &= \frac{1}{2\mathrm{i}kP}\iint\xi\left(\frac{\partial W(\xi_1,\eta_1;\xi_2,\eta_2;0)}{\partial\xi_2}-\frac{\partial W(\xi_1,\eta_1;\xi_2,\eta_2;0)}{\partial\xi_1}\right)\Bigg|_{\xi_1=\xi_2=\xi,\,\eta_1=\eta_2=\eta}\mathrm{d}\xi\,\mathrm{d}\eta\,,\\
\langle\eta v\rangle &= \frac{1}{2\mathrm{i}kP}\iint\eta\left(\frac{\partial W(\xi_1,\eta_1;\xi_2,\eta_2;0)}{\partial\eta_2}-\frac{\partial W(\xi_1,\eta_1;\xi_2,\eta_2;0)}{\partial\eta_1}\right)\Bigg|_{\xi_1=\xi_2=\xi,\,\eta_1=\eta_2=\eta}\mathrm{d}\xi\,\mathrm{d}\eta\,,
\end{aligned} \tag{13}$$

being P the total power of the beam, i.e.,

$$P = \iint W(\xi,\eta;\xi,\eta)\,\mathrm{d}\xi\,\mathrm{d}\eta\,. \tag{14}$$

Then, the rms width of the beam across a transverse plane and in the far field can be defined as $\sqrt{\langle\xi^2+\eta^2\rangle}=\sqrt{\langle\xi^2\rangle+\langle\eta^2\rangle}$ and $\sqrt{\langle u^2+v^2\rangle}=\sqrt{\langle u^2\rangle+\langle v^2\rangle}$, respectively, while the mixed second order moment $\langle\xi u+\eta v\rangle=\langle\xi u\rangle+\langle\eta v\rangle$ accounts for the curvature of the wavefront. These parameters allow to evaluate beam quality parameter defined as [54, 55]

$$Q = \left\langle\xi^2+\eta^2\right\rangle\left\langle u^2+v^2\right\rangle-\langle\xi u+\eta v\rangle^2\,, \tag{15}$$

that is invariant under propagation through rotationally symmetric ABCD optical systems and reaches the minimum value of $1/k^2$ for a coherent fundamental Gaussian beam. This parameter is related to the beam propagation factor, M^2, through the expression $M^2 = k\sqrt{Q}$. The Q parameter is a measure of the beam quality, where a better beam quality is associated with a

Optics EXPRESS

smaller divergence, for a fixed beam width at the source plane [54]. Due to the invariant character of Q, it can be evaluated at any transverse plane and this calculation is usually easier at the beam waist (located at $z = 0$ for our source), where $\langle \xi u + \eta v \rangle = 0$.

The expressions of the second-order moments and the quality factor can be performed analytically, after substituting the CSD given by Eq. (9) into Eqs. (13). In particular, the rms beam width turns out

$$\left\langle r^2 \right\rangle_z = \frac{w_0^2}{2}\left[1 + |m| + \left(\frac{z^2}{z_R^2}\right)\left(1 + \frac{w_0^2}{\delta_c^2} + |m|\right)\right], \tag{16}$$

where $z_R = kw_0^2/2$ is the Rayleigh length pertaining to a coherent Gaussian beam with waist size w_0 [52].

By substituting the calculated second order moments into Eq. (15), the beam quality factor is obtained as

$$Q = \frac{1 + |m|}{k^2}\left(1 + \frac{w_0^2}{\delta_c^2} + |m|\right). \tag{17}$$

The rms beam width and the quality factor Q can be also calculated for the equivalent standard Schell-model source described by Eq. (10). Following the same procedure, it turns out that [56,57]

$$\left\langle r^2 \right\rangle_z^{(\mathrm{s})} = \frac{w_0^2}{2}\left[1 + |m| + \left(\frac{z^2}{z_R^2}\right)\left(1 + \frac{2w_0^2}{\delta_c^2} + |m|\right)\right], \tag{18}$$

and

$$Q^{(\mathrm{s})} = \frac{1 + |m|}{k^2}\left(1 + \frac{2w_0^2}{\delta_c^2} + |m|\right). \tag{19}$$

The obtained expressions are very similar, the only difference being the factor 2 multiplying the ratio w_0^2/δ_c^2 in the latter. This means that a Gaussian pseudo-Schell-model beam has a better quality and diverges less than the corresponding standard GSM beam. More precisely, with the same parameters, it diverges like a standard GSM beam with coherence area increased by a factor 2.

Figure 3 shows the evolution of the rms beam width along the z axis and the beam quality factor Q for different values of the topological charge m (including the case $m = 0$). The results are compared to those of a GSM source with the same waist size w_0 and coherence parameter δ_c.

Additional advantages of the sources introduced here over the equivalent GSM sources are related to the irradiance profile in free space propagation. Then, the evolution of the irradiance profile will be analyzed in Section 5. Numerical results will be shown in detail for the cases $m = 0$ and $m = 1$.

5. Irradiance of the propagated field

5.1. Gaussian pseudo Schell-model sources

In this case, the irradiance at the source plane corresponds to that of a Gaussian with spot size w_0. It is well known that the irradiance profile of a standard GSM beam remains invariant, except for a scale factor, in free space propagation [28, 29]. However, the irradiance profile of the generated beam by a GPSM source changes upon free propagation in a way that depends on the selected coherence parameter δ_c in Eq. (7).

As an example, Fig. 4 shows the evolution of the irradiance at several propagation distances for $\delta_c = 0.2w_0$. A somewhat unexpected behavior is found: in a certain range of propagation

Optics EXPRESS

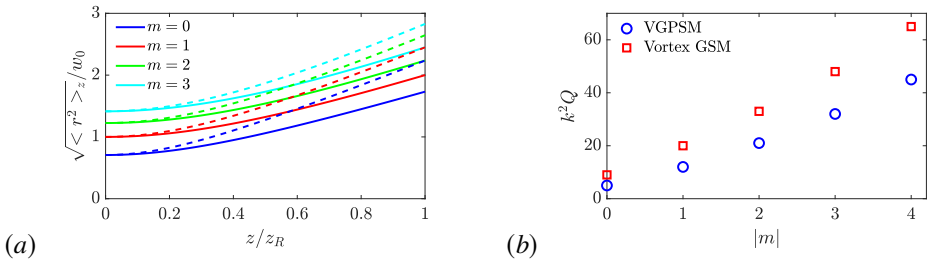

Fig. 3. (a) Evolution of rms beam width along propagation distance and (b) quality factor for different values of m and $\delta_c = w_0/2$. For comparison purposes the same quantities for the corresponding GSM or VGSM beams are also shown (dashed lines and squares).

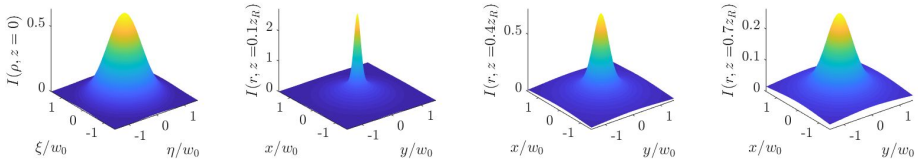

Fig. 4. Irradiance profile of a GPSM at $z = 0$, $z = 0.1z_R$, $z = 0.4z_R$, and $z = 0.7z_R$, from left to right for a coherence parameter $\delta_c = 0.2w_0$.

distances, the irradiance profile becomes narrower and presents a maximum value higher than that at the beam waist (note that the vertical scale in each part of Fig. 4 is different).

In order to analyze in a deeper detail such a behavior, the transverse shape of the irradiance (normalized to its maximum value) as a function of the radial coordinate ρ is shown in Fig. 5(a). In general, it is Gaussian only at the source plane but it evolves during propagation in a way depending on the coherence parameter δ_c. In particular, for coherence parameters smaller than the waist size and short propagation distances, it presents a shoulder. But the most significant aspect is that during propagation the profile becomes sharper than that at the source plane. For the chosen values of the parameters, the maximum sharpness is reached at a distance of the order of $z_R/5$.

Figure 5(b) reports the transverse full width at half maximum (FWHM) as a function of the propagation distance for different values of the coherence parameter δ_c. It clearly shows the sharpening of the transverse irradiance occurring during propagation when δ_c is lower than w_0, thus confirming what we already noticed in Fig. 5(a). This minimum FWHM is smaller and nearer to the source plane for lower and lower values of the coherence width across the source.

It should be stressed that such a result does not contradict the fact that the width of the beam, defined in terms of the second-order moment of the intensity profile, presents its minimum value at the source plane and then increases monotonically with z, as shown in Sec. 4 (see Eq. (16)). Actually, the smaller the coherence parameter, the faster the increasing of the rms width of the beam profile. The variance of the profile, indeed, also depends on the irradiance at points very far away from the center and, in some cases does not carry the same information as the transverse FWHM plotted in Fig. 5(b). For example, the curves in Fig. 5(a) corresponding to $z = 0$ and to $z = 0.7\, z_R$ seem to correspond to quite similar values of the FWHM. For the latter, however, the tail is higher, and this gives rise to a greater value of the variance.

Figure 6 shows the behavior of the maximum value of the transverse irradiance profile (which, in this case, is found at the beam center) as a function of the propagation distance, for several

Optics EXPRESS

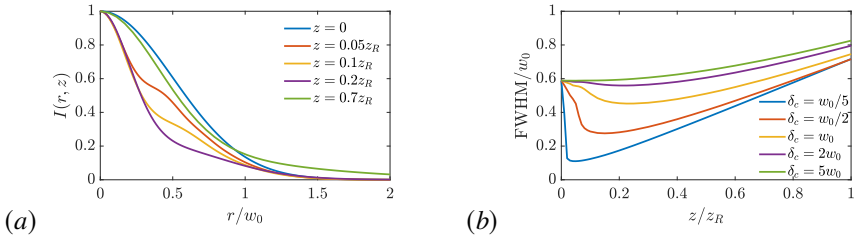

Fig. 5. (a) Normalized irradiance profile at different propagation distances for $\delta_c = w_0/2$ and (b) evolution of the FWHM of the beam with propagation distance for several values of the coherence parameter for a GPSM source.

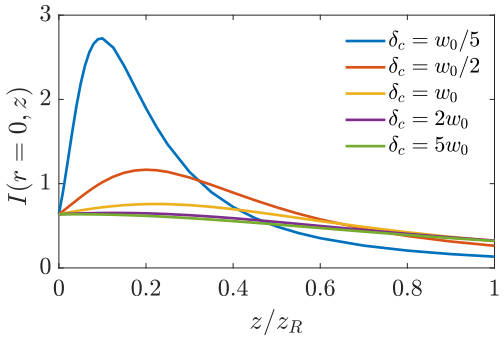

Fig. 6. Maximum irradiance of a GPSM beam during propagation for several values of the coherence parameter.

values of the coherence parameter δ_c. It can be noted that for large values of δ_c the maximum irradiance reduces monotonically with propagation, in a way quite similar to that occurring for a GSM beam. On the contrary, for lower values of the coherence parameter (of the order or smaller than w_0), the axial irradiance presents a peak, at distances of the order of $z_R/2$ or less from the source, where its value is greater than that at the source plane. The peak value of the maximum irradiance increases and the distance at which its maximum is reached decreases on decreasing the coherence parameter δ_c.

Similar sharpening of the beam profile have been already described for some partially coherent sources with non shift invariant coherence characteristics [6, 9, 44].

5.2. *Vortex Gaussian pseudo Schell-model sources with m=1*

In the next example we will consider a Gaussian vortex with topological charge $m = 1$, i.e., the $\tau(\boldsymbol{\rho})$ function in Eq. (8) evaluated for $m = 1$.

The irradiance profile at the source plane in this case corresponds to the shape of a usual coherent Laguerre-Gaussian beam of zero order and with topological charge $m = 1$ as it can be seen in the upper left part of Fig. 7. However, due to the coherence characteristics imposed to the source, the irradiance profile of the propagated beam may present some interesting feature.

First of all, the irradiance is zero everywhere along the beam axis, as it can be seen from Eq. (12), because the Bessel functions J_m in the integral vanish for $r_1 = 0$ and $r_2 = 0$ (if $m \neq 0$), so that the donut-like shape is preserved during propagation. This is not the case for usual partially coherent hollow beams of the Schell-model type [58–60]. Furthermore, as we shall see, the irradiance profile of the propagated beam at certain planes may be much narrower than that

Optics EXPRESS

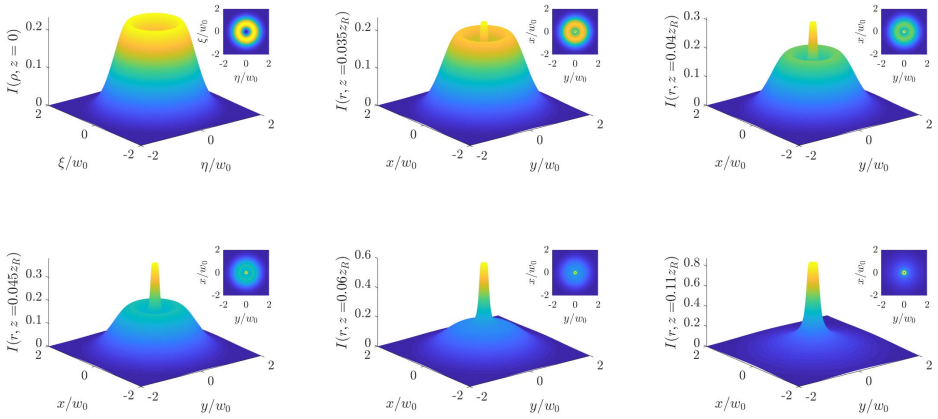

Fig. 7. Evolution of the irradiance at several distances for the case of a VGPSM source with topological charge $m = 1$ and coherence parameter $\delta_c = w_0/8$.

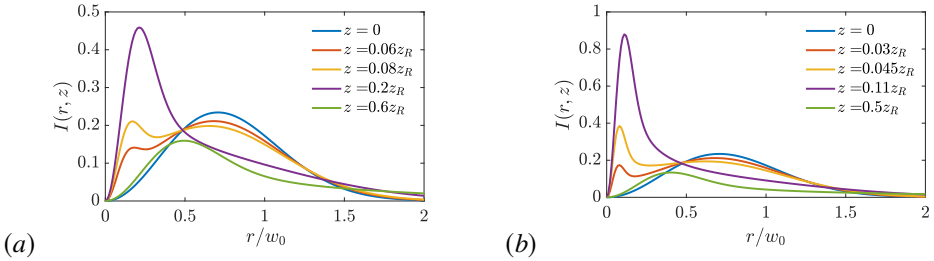

Fig. 8. Irradiance profile at several distances for the case of a VGPSM source with topological charge $m = 1$ and (a) $\delta_c = w_0/4$; (b) $\delta_c = w_0/8$.

across the source. As a consequence, the maximum irradiance value of the propagated beam may be much higher than that at the source plane.

The evolution of the transverse profile during propagation is quite complex and is shown in Fig. 7. Close to the plane $z = 0$, the profile is very similar to that of the source but after a certain propagation distance a second, smaller donut appear around the beam axis, which gradually becomes predominant. This behavior is made evident in Fig. 8, where the transverse profile is shown as a function of the radial coordinate for different values of δ_c. It appears that the transverse size of the second donut depends on the coherence parameter of the source. A consequence of such a behavior is that the FWHM of the beam (defined as the largest value of the radius at which the irradiance reaches the half of its maximum) is not monotonic with the propagation distance (see Fig. 9) but presents an abrupt reduction at a propagation distance that depends on the coherence parameter. This effect becomes more and more evident on reducing the value of the coherence parameter and could be used in particle trapping, due to the small confinement region and the large gradient of the irradiance in the region where the inner donut appears.

The behavior of the maximum irradiance of the beam profile during propagation is shown in Fig. 10. It can be traced back to the one of the beam width, being related to the peculiar way in which the profile of the irradiance evolves for relatively low values of the coherence parameter δ_c, as it was shown in Figs. 7 and 10.

Optics EXPRESS

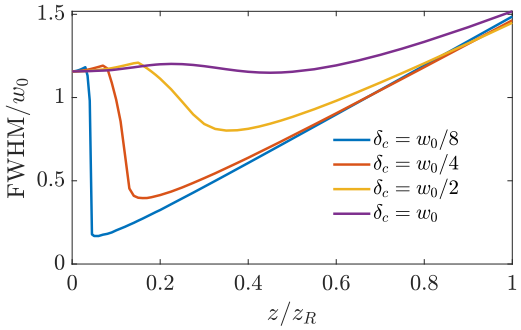

Fig. 9. Evolution of the FWHM of the irradiance profile of the beam radiated from a VGPSM source with topological charge $m = 1$, as a function of the propagation distance for several values of the coherence parameter δ_c.

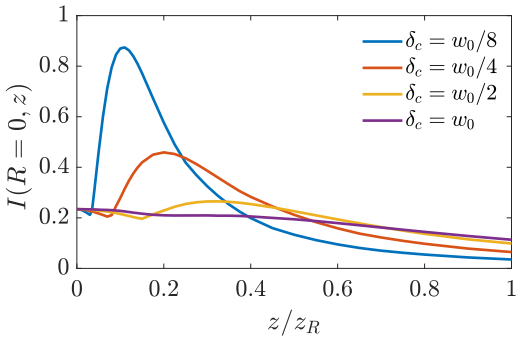

Fig. 10. Evolution with propagation distance of the maximum irradiance at each transverse plane, for the case of a VGPSM source with topological charge $m = 1$ and several values of the coherence parameter δ_c.

6. Synthesis

The CSD function of any source can be expressed by means of the following Mercer expansion:

$$W(\boldsymbol{\rho}_1, \boldsymbol{\rho}_2) = \sum_{n=0}^{\infty} \lambda_n \Psi_n^*(\boldsymbol{\rho}_1) \Psi_n(\boldsymbol{\rho}_2) \tag{20}$$

where λ_n are positive coefficients (the eigenvalues) and the functions $\Psi_n(\boldsymbol{\rho})$ (the modes) form a set of orthonormal functions [1, 61]. Sometimes, expansions of the form (20) are also possible with positive coefficients and nonorthogonal functions. In such cases, the latter are called pseudo-modes [34, 62]. In both cases, the physical meaning of the above expansion is that a partially coherent source can be thought of as the superposition of a set of mutually uncorrelated, perfectly coherent, and suitably weighted fields. Of course, this also represents a way to physically synthesize partially coherent source [19, 22, 23, 26, 40, 63], especially when they are not of the Schell-model type [6, 44, 45]. The superposition usually involves an infinite number of coherent fields but for practical applications a finite number is often enough for a good representation of the CSD function [27, 44].

Using a known result obtained for the case of a 1D GSM source [27, 64], the following

Optics EXPRESS

expansion can be derived for the CSD in Eq. (9):

$$W_m(\boldsymbol{\rho}_1, \boldsymbol{\rho}_2, 0) = A_0 \sum_{n=0}^{\infty} \frac{\gamma^n}{2^n n!} \psi^*_{m,n}(\boldsymbol{\rho}_1) \psi_{m,n}(\boldsymbol{\rho}_2), \tag{21}$$

where

$$\gamma = \left[1 + \frac{\delta_c^2}{w_0^2} + \frac{\sqrt{2}\delta_c}{w_0} \left(1 + \frac{\delta_c^2}{2w_0^2} \right)^{1/2} \right]^{-1}, \tag{22}$$

and

$$\psi_{m,n}(\boldsymbol{\rho}) = \left(\frac{\sqrt{2}\,\rho}{w_0} \right)^m \exp(\mathrm{i}m\varphi) H_n\left(\sqrt{2\alpha}\,\rho \right) \exp\left(-\alpha\,\rho^2 \right), \tag{23}$$

being $H_n(\cdot)$ the Hermite polynomial of order n [51], and

$$\alpha = \frac{1}{w_0^2} \left(1 + \frac{2w_0^2}{\delta_c^2} \right)^{1/2}. \tag{24}$$

In general, the functions $\psi_{m,n}$ are not orthogonal in 2D, and they neither are normalized. But we can define a set of pseudo-modes by introducing the normalized functions

$$\Psi_{m,n}(\boldsymbol{\rho}) = \frac{1}{\beta_{m,n}} \psi_{m,n}(\boldsymbol{\rho}), \tag{25}$$

where $\beta_{m,n}$ is such that

$$\begin{aligned} \beta_{m,n}^2 &= 2\pi \int_0^{\infty} \left(\frac{2\,\rho}{w_0} \right)^{2m} H_n^2\left(\sqrt{2\gamma}\,\rho \right) \exp\left(-2\gamma\,\rho^2 \right) \rho\,\mathrm{d}\rho \\ &= \frac{2^{2n-2m-2}\pi^{3/2}(2m+1)!}{w_0^{2m}\alpha^{m+1}\Gamma(m-n+3/2)} {}_2F_1(-n, -n; m-n+3/2; 1/2), \end{aligned} \tag{26}$$

and ${}_2F_1$ is the generalized hypergeometric function [65].

Therefore, a pseudo-modal expansion for W_m can be written in the form (see Eqs. (21) and (25))

$$W_m(\boldsymbol{\rho}_1, \boldsymbol{\rho}_2, 0) = A_0 \sum_{n=0}^{\infty} \lambda_{m,n} \Psi^*_{m,n}(\boldsymbol{\rho}_1) \Psi_{m,n}(\boldsymbol{\rho}_2), \tag{27}$$

where the coefficients $\lambda_{m,n}$ are

$$\lambda_{m,n} = \frac{\gamma^n}{2^n n!} \beta_{m,n}^2. \tag{28}$$

For the case of GPSM source, the behavior of the coefficients $\lambda_{0,n}$ for $n = 0$ to $n = 10$ is shown in Fig. 11 as a function of the ratio of coherence parameter δ_c to the beam width at its waist. It can be observed that when this ratio is large, for example $\delta_c/w_0 > 4$, the source is highly coherent and then the contribution of only two modes could be enough to represent the source. However, when this ratio decreases so the source becomes more and more incoherent, it is necessary to take into account the contribution of more and more pseudo-modes. For example, in the inset can be observed that for a ratio $\delta_c/w_0 < 1/2$ more than ten modes are needed to accurately represent the source.

For the case of VGPSM, the coefficients $\lambda_{m,n}$ present a similar behavior. However, for a given value of the δ_c/w_0, a higher number of modes is necessary to accurately represent the source,

Optics EXPRESS

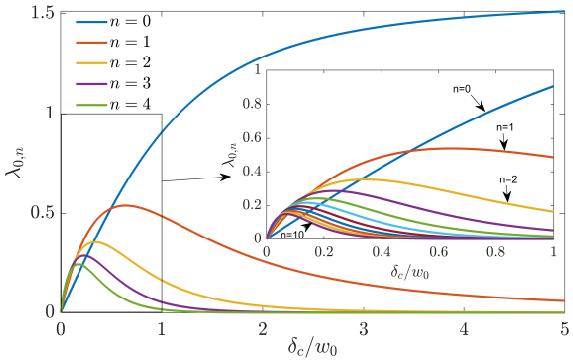

Fig. 11. Coefficients of the pseudo-modal expansion for the GPSM source as a function of the coherence parameter δ_c.

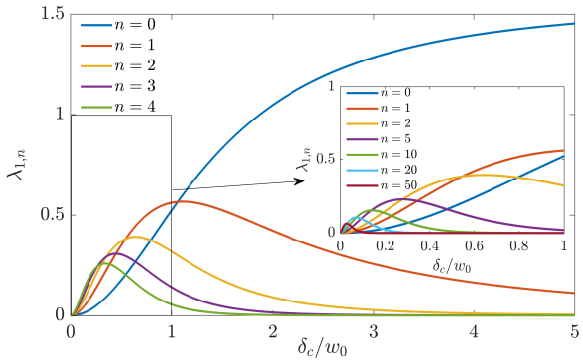

Fig. 12. Coefficients of the pseudo-modal expansion for the VGPSM source as a function of the coherence parameter δ_c.

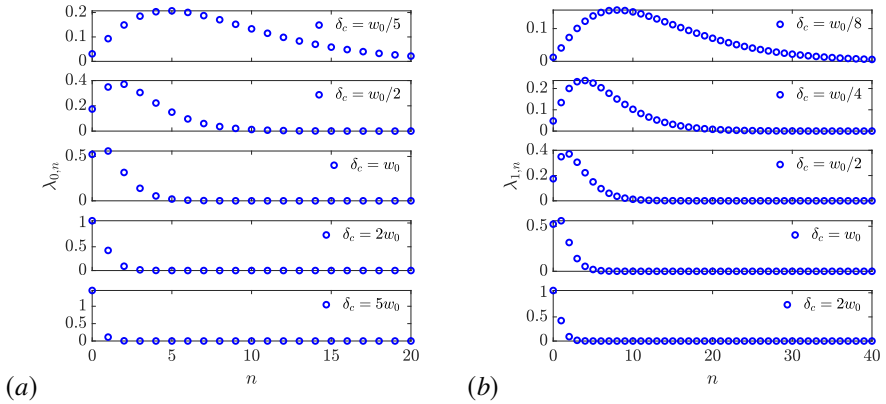

(*a*) (*b*)

Fig. 13. Coefficients of the pseudo-modal expansion for (a) the GPSM and (b) VGPSM source for different values of the coherence parameter δ_c.

Optics EXPRESS

specially for lower and lower values of such a ratio. This can be deduced from observing Fig. 12 where it can be observed that, for example, the coefficient $\lambda_{1,50}$ shows a greater value for δ_c/w_0 around 0.05 than the lower order modes.

Figure 13 shows the set of the first 21 (41) coefficients for GPSM (VGPSM) sources with different values of δ_c/w_0 ratio. It can be noted that for highly coherent GPSM and VGPSM sources, the most significant contribution is that of the zero-th order mode. On the other hand, for lower and lower coherence, the most important contribution to the source comes from higher and higher order modes.

7. Conclusion

In the present work, a type of partially coherent sources is proposed and analyzed. Sources of this kind present a degree of coherence that is radially shift invariant, so that points at the same distance from the source center are perfectly coherent, but the coherence generally decreases for points on circles of different radii. This radial shift-invariance makes the coherence area growing with the distance from the source center. Pseudo-Schell model sources with Laguerre-Gaussian irradiance profile and Gaussian degree of coherence have been studied in detail. Beams radiated from sources of this kind show better beam quality parameters than equivalent Schell-model beams with comparing parameters. An interesting property of the propagated beams is that, at certain distances, the FWHM of their irradiance profile can be significantly smaller than that at the beam waist. Furthermore, when the irradiance profile presents a null at the source center, the irradiance of the radiated beam remains equal to zero at the beam axis for any propagation distance, giving rise to a dark hollow partially coherent beam. The above properties could be exploited for particle trapping, due to the great irradiance gradient obtained in the radial direction. Finally, a pseudo-modal expansion of the CSD has been derived, which allows to build up the source with an adequate superposition of pseudo modes.

Funding

Spanish Ministerio de Economía y Competitividad (FIS2016-75147).

References

1. L. Mandel and E. Wolf, *Optical Coherence and Quantum Optics* (Cambridge University, 1995).
2. G. Gbur and T. D. Visser, "Can spatial coherence effects produce a local minimum of intensity at focus?," Opt. Lett. **28**, 1627–1629 (2003).
3. J. Pu, S. Nemoto, and X. Liu, "Beam shaping of focused partially coherent beams by use of the spatial coherence effect," Appl. Opt. **43**, 5281–5286 (2004).
4. T. van Dijk, G. Gbur, and T. D. Visser, "Shaping the focal intensity distribution using spatial coherence," J. Opt. Soc. Am. A **25**, 575–581 (2008).
5. T. van Dijk, D. G. Fischer, T. D. Visser, and E. Wolf, "Effects of spatial coherence on the angular distribution of radiant intensity generated by scattering on a sphere," Phys. Rev. Lett. **104**, 173902 (2010).
6. H. Lajunen and T. Saastamoinen, "Propagation characteristics of partially coherent beams with spatially varying correlations," Opt. Lett. **36**, 4104–4106 (2011).
7. S. Sahin and O. Korotkova, "Light sources generating far fields with tunable flat profiles," Opt. Lett. **37**, 2970–2972 (2012).
8. M. Singh, J. Tervo, and J. Turunen, "Elementary-field analysis of partially coherent beam shaping," J. Opt. Soc. Am. A **30**, 2611–2617 (2013).
9. C. Ding, M. Koivurova, J. Turunen, and L. Pan, "Self-focusing of a partially coherent beam with circular coherence," J. Opt. Soc. Am. A **34**, 1441–1447 (2017).
10. G. Wu and Y. Cai, "Detection of a semirough target in turbulent atmosphere by a partially coherent beam," Opt. Lett. **36**, 1939–1941 (2011).
11. J. C. Ricklin and F. M. Davidson, "Atmospheric turbulence effects on a partially coherent Gaussian beam: implications for free-space laser communication," J. Opt. Soc. Am. A **19**, 1794–1802 (2002).
12. O. Korotkova, L. C. Andrews, and R. L. Phillips, "Model for a partially coherent Gaussian beam in atmospheric turbulence with application in lasercom," Opt. Eng. **43**, 330 – 341 (2004).
13. G. Gbur, "Partially coherent beam propagation in atmospheric turbulence [invited]," J. Opt. Soc. Am. A **31**, 2038–2045 (2014).

Optics EXPRESS

14. S. B. Raghunathan, T. van Dijk, E. J. G. Peterman, and T. D. Visser, "Experimental demonstration of an intensity minimum at the focus of a laser beam created by spatial coherence: application to the optical trapping of dielectric particles," Opt. Lett. **35**, 4166–4168 (2010).
15. C. Zhao and Y. Cai, "Trapping two types of particles using a focused partially coherent elegant Laguerre–Gaussian beam," Opt. Lett. **36**, 2251–2253 (2011).
16. F. Gori, G. Guattari, and C. Padovani, "Modal expansion for J0-correlated Schell-model sources," Opt. Commun. **64**, 311–316 (1987).
17. F. Gori, M. Santarsiero, R. Borghi, and C.-F. Li, "Partially correlated thin annular sources: the scalar case," J. Opt. Soc. Am. A **25**, 2826–2832 (2008).
18. F. Gori, M. Santarsiero, R. Borghi, and S. Vicalvi, "Partially coherent sources with helicoidal modes," J. Mod. Opt. **45**, 539–554 (1998).
19. F. Wang and Y. Cai, "Experimental generation of a partially coherent flat-topped beam," Opt. Lett. **33**, 1795–1797 (2008).
20. O. Korotkova, S. Sahin, and E. Shchepakina, "Multi-Gaussian Schell-model beams," J. Opt. Soc. Am. A **29**, 2159–2164 (2012).
21. Z. Mei and O. Korotkova, "Cosine-Gaussian Schell-model sources," Opt. Lett. **38**, 2578–2580 (2013).
22. Y. Chen, S.A. Ponomarenko, and Y. Cai, "Experimental generation of optical coherence lattices," Appl. Phys. Lett. **109**, 061107 (2016).
23. Y. Chen, S.A. Ponomarenko, and Y. Cai, "Self-steering partially coherent beams," Scientific Reports **7** 39957 (2017).
24. E. Collett and E. Wolf, "Is complete spatial coherence necessary for the generation of highly directional light beams?," Opt. Lett. **2**, 27–29 (1978).
25. R. Martínez-Herrero, "Expansion of complex degree of coherence," Nuovo Cimento B **54**, 205–210 (1979).
26. P. D. Santis, F. Gori, G. Guattari, and C. Palma, "An example of a Collett-Wolf source," Opt. Commun. **29**, 256 – 260 (1979).
27. F. Gori, "Collett-Wolf sources and multimode lasers," Opt. Commun. **34**, 301 – 305 (1980).
28. A. T. Friberg and R. J. Sudol, "Propagation parameters of Gaussian Schell-model beams," Opt. Commun. **41**, 383 – 387 (1982).
29. F. Gori, "Mode propagation of the field generated by Collett-Wolf Schell-model sources," Opt. Commun. **46**, 149 – 154 (1983).
30. R. Martínez-Herrero and P. M. Mejías, "Radiometric definitions for partially coherent sources," J. Opt. Soc. Am. A **1**, 556–558 (1984).
31. J. Serna, P. Mejías, and R. Martínez-Herrero, "Beam quality dependence on the coherence length of Gaussian Schell-model fields propagating through ABCD optical systems," J. Mod. Opt. **39**, 625–635 (1992).
32. E. Tervonen, J. Turunen, and A. T. Friberg, "Gaussian Schell-model beams generated with synthetic acousto-optic holograms," J. Opt. Soc. Am. A **9**, 796–803 (1992).
33. F. Gori and M. Santarsiero, "Devising genuine spatial correlation functions," Opt. Lett. **32**, 3531–3533 (2007).
34. R. Martínez-Herrero, P. M. Mejías, and F. Gori, "Genuine cross-spectral densities and pseudo-modal expansions," Opt. Lett. **34**, 1399–1401 (2009).
35. C. Liang, F. Wang, X. Liu, Y. Cai, and O. Korotkova, "Experimental generation of cosine-Gaussian-correlated Schell-model beams with rectangular symmetry," Opt. Lett. **39**, 769–772 (2014).
36. Z. Mei, Y. Mao, and Y. Wang, "Electromagnetic multi-Gaussian Schell-model vortex light sources and their radiation field properties," Opt. Express **26**, 21992–22000 (2018).
37. Y. Cai, Y. Chen, and F. Wang, "Generation and propagation of partially coherent beams with nonconventional correlation functions: a review [invited]," J. Opt. Soc. Am. A **31**, 2083–2096 (2014).
38. M. Santarsiero, G. Piquero, J. C. G. de Sande, and F. Gori, "Difference of cross-spectral densities," Opt. Lett. **39**, 1713–1716 (2014).
39. J. C. G. de Sande, M. Santarsiero, G. Piquero, and F. Gori, "The subtraction of mutually displaced Gaussian Schell-model beams," J. Opt. **17**, 125613 (2015).
40. M. W. Hyde IV, S. R. Bose-Pillai, and R. A. Wood, "Synthesis of non-uniformly correlated partially coherent sources using a deformable mirror," Appl. Phys. Lett. **111**, 101106 (2017).
41. M. Santarsiero, R. Martínez-Herrero, D. Maluenda, J. C. G. de Sande, G. Piquero, and F. Gori, "Partially coherent sources with circular coherence," Opt. Lett. **42**, 1512–1515 (2017).
42. M. Santarsiero, R. Martínez-Herrero, D. Maluenda, J. C. G. de Sande, G. Piquero, and F. Gori, "Synthesis of circularly coherent sources," Opt. Lett. **42**, 4115–4118 (2017).
43. Y. Cai, Y. Chen, J. Yu, X. Liu, and L. Liu, "Generation of partially coherent beams," Prog. Opt. **62**, 157–223 (2017).
44. D. Wu, F. Wang, and Y. Cai, "High-order nonuniformly correlated beams," Opt. Laser Technol. **99**, 230 – 237 (2018).
45. G. Piquero, M. Santarsiero, R. Martínez-Herrero, J. C. G. de Sande, M. Alonzo, and F. Gori, "Partially coherent sources with radial coherence," Opt. Lett. **43**, 2376–2379 (2018).
46. R. Martínez-Herrero, D. Maluenda, G. Piquero, and J. C. G. de Sande, "Vortex pseudo Schell-model source: A proposal," in "2016 15th Workshop on Information Optics (WIO)," (2016), pp. 1–3.
47. G. Piquero, P. M. Mejías, and R. Martínez-Herrero, "Quality changes of Gaussian beams propagating through axicons," Opt. Commun. **105**, 289–291 (1994).
48. A. V. Ustinov and S. N. Khonina, "Calculating the complex transmission function of refractive axicons," Opt. Mem.

Optics EXPRESS

Neural Networks **21**, 133–144 (2012).
49. F. Gori, M. Santarsiero, R. Borghi, and V. Ramírez-Sánchez, "Realizability condition for electromagnetic Schell-model sources," J. Opt. Soc. Am. A **25**, 1016–1021 (2008).
50. R. Martínez-Herrero and P. M. Mejías, "Elementary-field expansions of genuine cross-spectral density matrices," Opt. Lett. **34**, 2303–2305 (2009).
51. M. Abramowitz and I. Stegun, eds., *Handbook of mathematical functions* (Dover Publications Inc, 1972).
52. A. E. Siegman, *Lasers* (University Science Books, 1986).
53. D. M. Palacios, I. D. Maleev, A. S. Marathay, and G. A. Swartzlander, "Spatial correlation singularity of a vortex field," Phys. Rev. Lett. **92**, 143905 (2004).
54. J. Serna, R. Martínez-Herrero, and P. M. Mejías, "Parametric characterization of general partially coherent beams propagating through ABCD optical systems," J. Opt. Soc. Am. A **8**, 1094–1098 (1991).
55. R. Martínez-Herrero, P. M. Mejías, and G. Piquero, "Quality improvement of partially coherent symmetric-intensity beams caused by quartic phase distortions," Opt. Lett. **17**, 1650–1651 (1992).
56. M. Santarsiero, F. Gori, R. Borghi, G. Cincotti, and P. Vahimaa, "Spreading properties of beams radiated by partially coherent Schell-model sources," J. Opt. Soc. Am. A **16**, 106–112 (1999).
57. W. Li, G. Feng, and S. Zhou, "The M^2 factor matrix of a paraxial Laguerre-Gaussian beam," J. Mod. Opt. **60**, 704–712 (2013).
58. Y. Cai, X. Lu, and Q. Lin, "Hollow Gaussian beams and their propagation properties," Opt. Lett. **28**, 1084–1086 (2003).
59. X. Lü and Y. Cai, "Partially coherent circular and elliptical dark hollow beams and their paraxial propagations," Phys. Lett. A **369**, 157 – 166 (2007).
60. L.-G. Wang and L.-Q. Wang, "Hollow Gaussian Schell-model beam and its propagation," Opt. Commun. **281**, 1337 – 1342 (2008).
61. E. Wolf, "New theory of partial coherence in the space–frequency domain. Part I: spectra and cross spectra of steady-state sources," J. Opt. Soc. Am. **72**, 343–351 (1982).
62. L. Ma and S. A. Ponomarenko, "Free-space propagation of optical coherence lattices and periodicity reciprocity," Opt. Express **23**, 1848–1856 (2015).
63. B. Rodenburg, M. Mirhosseini, O. S. Magaña-Loaiza, and R. W. Boyd, "Experimental generation of an optical field with arbitrary spatial coherence properties," J. Opt. Soc. Am. B **31**, A51–A55 (2014).
64. A. Starikov and E. Wolf, "Coherent-mode representation of Gaussian Schell-model sources and of their radiation fields," J. Opt. Soc. Am. **72**, 923–928 (1982).
65. A. Prudnikov, I. Brychkov, and O. Marichev, *Integrals and Series: Special functions* (Gordon and Breach Science Publishers, 1986).